Biophysical Journal, Volume *112*

Supplemental Information

Epithelial Folding Driven by Apical or Basal-Lateral Modulation: Geometric Features, Mechanical Inference, and Boundary Effects

Fu-Lai Wen, Yu-Chiun Wang, and Tatsuo Shibata

SUPPORTING MATERIAL

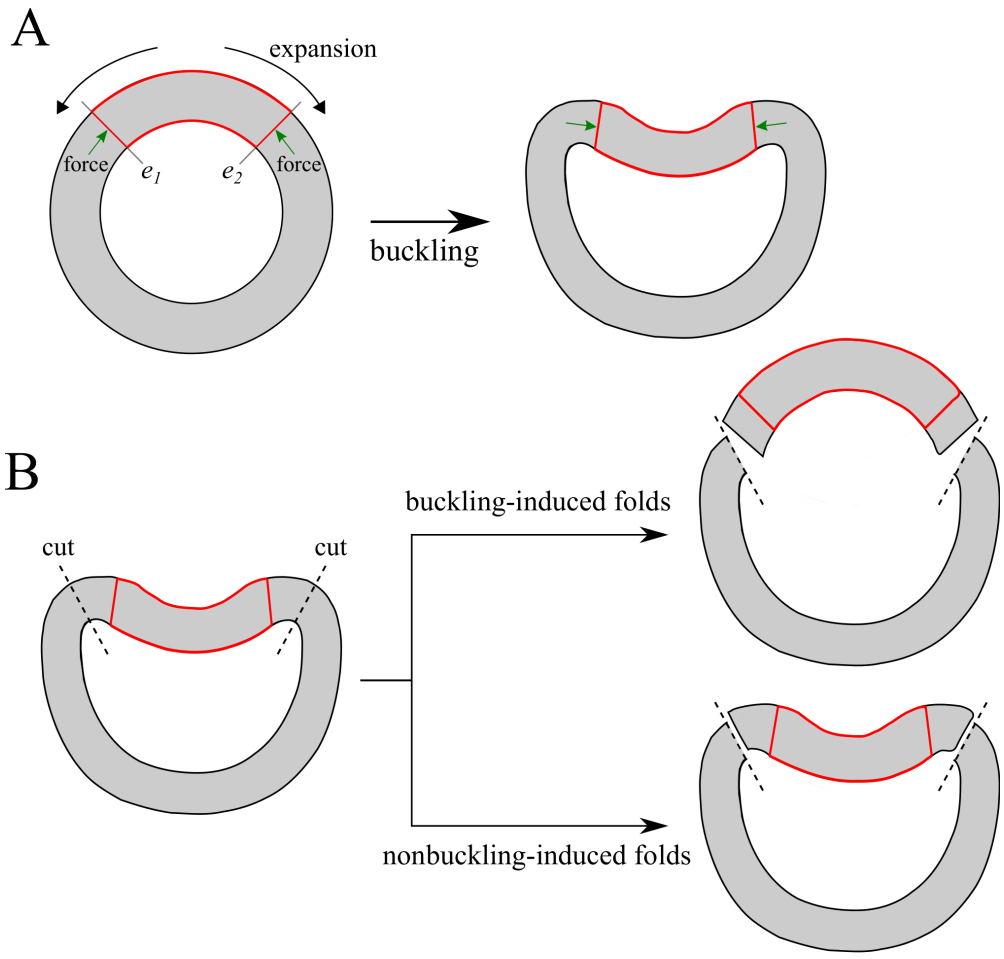

FIG. S1. Schematic illustration of fold formation in spherical/cylindrical epithelia (cross-sections shown in gray). (A) The expansion of a localized tissue area (red box) at one end e_1 is restricted by the expansion at the other end e_2 because of the looped structures. The increasing compressive stresses on the swelling area can cause folding via buckling instability. (B) Fold formation could result from buckling or non-buckling mechanisms. When the epithelial folds are formed via buckling instability, the shape of the folded area cannot be maintained if it is isolated from the epithelia. In contrast, the folds generated by a non-buckling mechanism can still maintain their shape even when they are excised from the main tissue body.

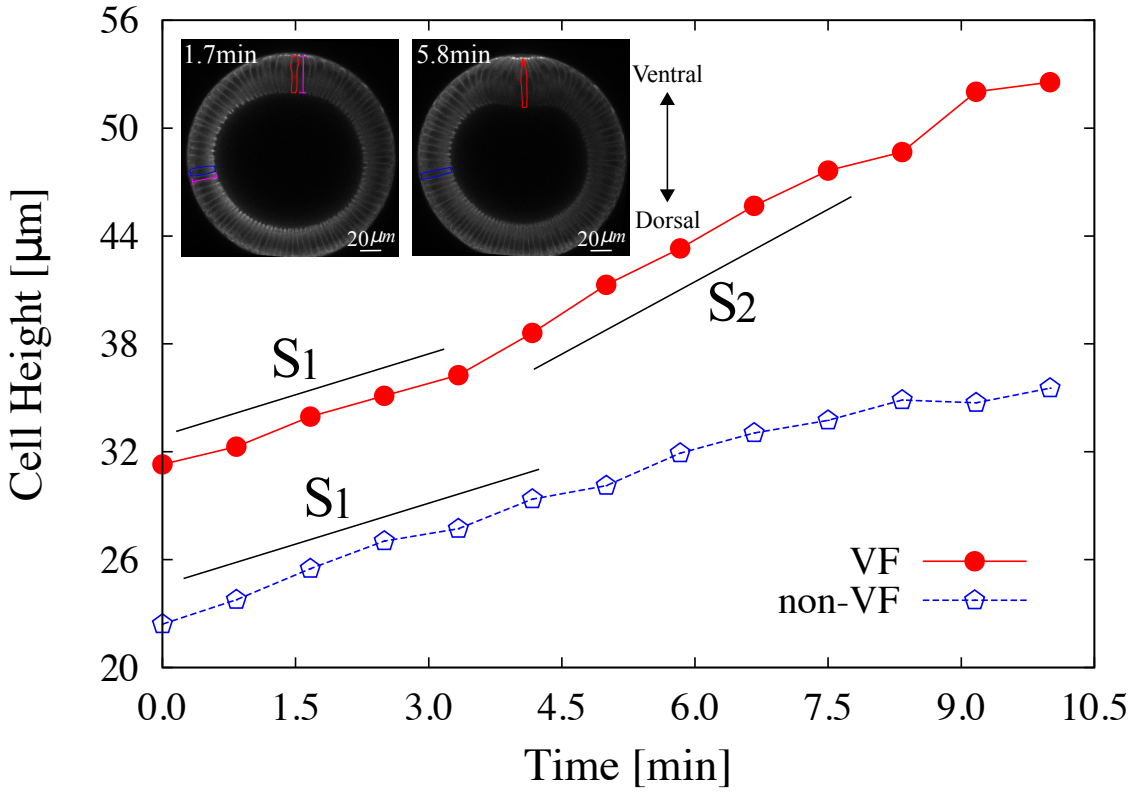

FIG. S2. Measurements of cell height during early *Drosophila* ventral furrow formation. The height of the ventral furrow (VF) cells, which actively contract their apical surfaces, and the surrounding passive cells (non-VF) are temporally traced from time-lapse imaging of the *Drosophila* embryos (WT3 in Fig. 4). The initial time point is chosen arbitrarily before the start of apical constriction of VF cells. Both the heights of VF and non-VF cells increase over time with the rate $S_1 = 1.54\mu$m/min, because of the morphological event called cellularization. At a later time stage, in addition to the cellularization, the action of apical constriction significantly increases the rate of change of cell height to $S_2 = 2.7\mu$m/min in the VF cells. See Appendix D for details of the experimental setup.

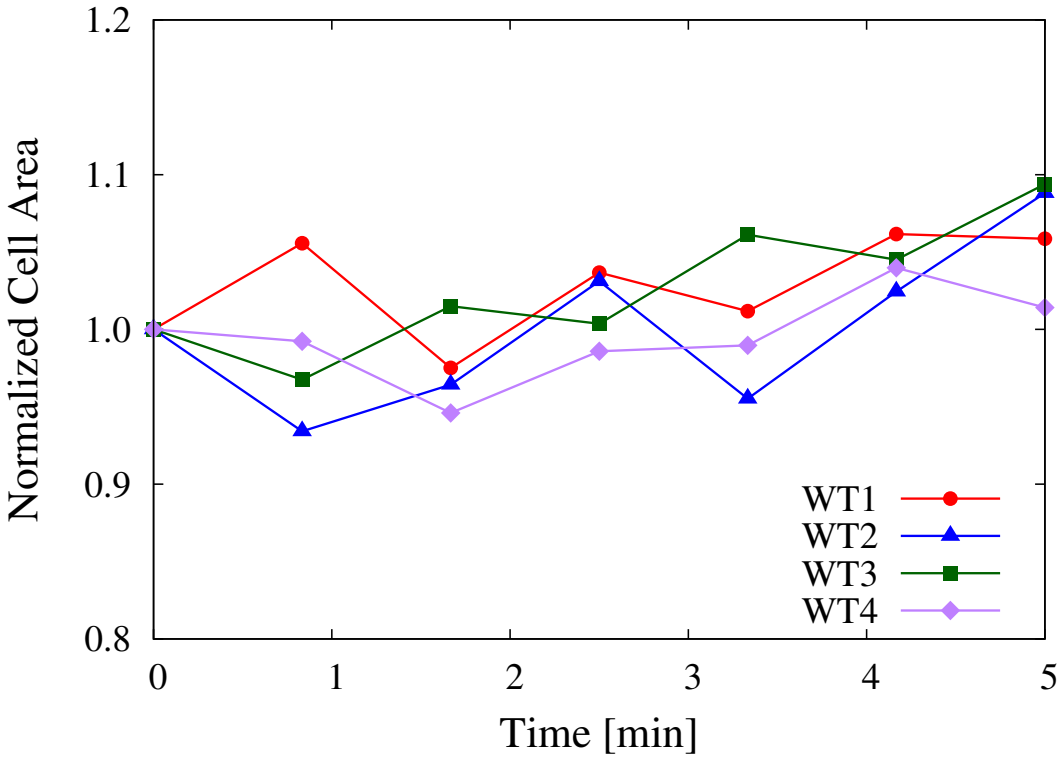

FIG. S3. Measurements of cross-sectional area of ventral furrow cells (cf. red box in the inset of Fig. S2) during early *Drosophila* ventral furrow formation. The data points, which are normalized by the initial point $t = 0$, are analyzed during the time interval that was used for the parameter estimation in Fig. 5. At the initial stage of furrow formation, the cross-sectional cell area exhibits only small fluctuations (less than ten percent) despite significant cell shape changes. See Appendix D for details of the experimental setup.

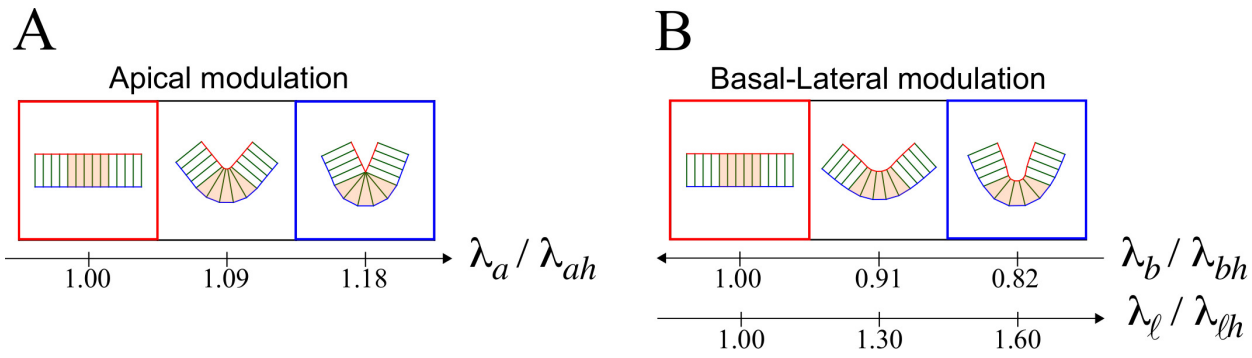

FIG. S4. Epithelial folding for the linear line tension model, where the apical mechanics is described by the line tension λ_a. The cells at the center ($N_c = 5$, colored by orange) of the sheet ($N = 13$) are mechanically modulated at the apical (A) or basal–lateral (B) surfaces. The flat sheet (red box) is generated at parameter values as those shown at the center of Fig. 1C with $\lambda_a = \lambda_b$. Note that the different modulation mechanisms sculpt epithelia into distinct folds (blue box) similar to those observed in our model considering the effect of apical elasticity.

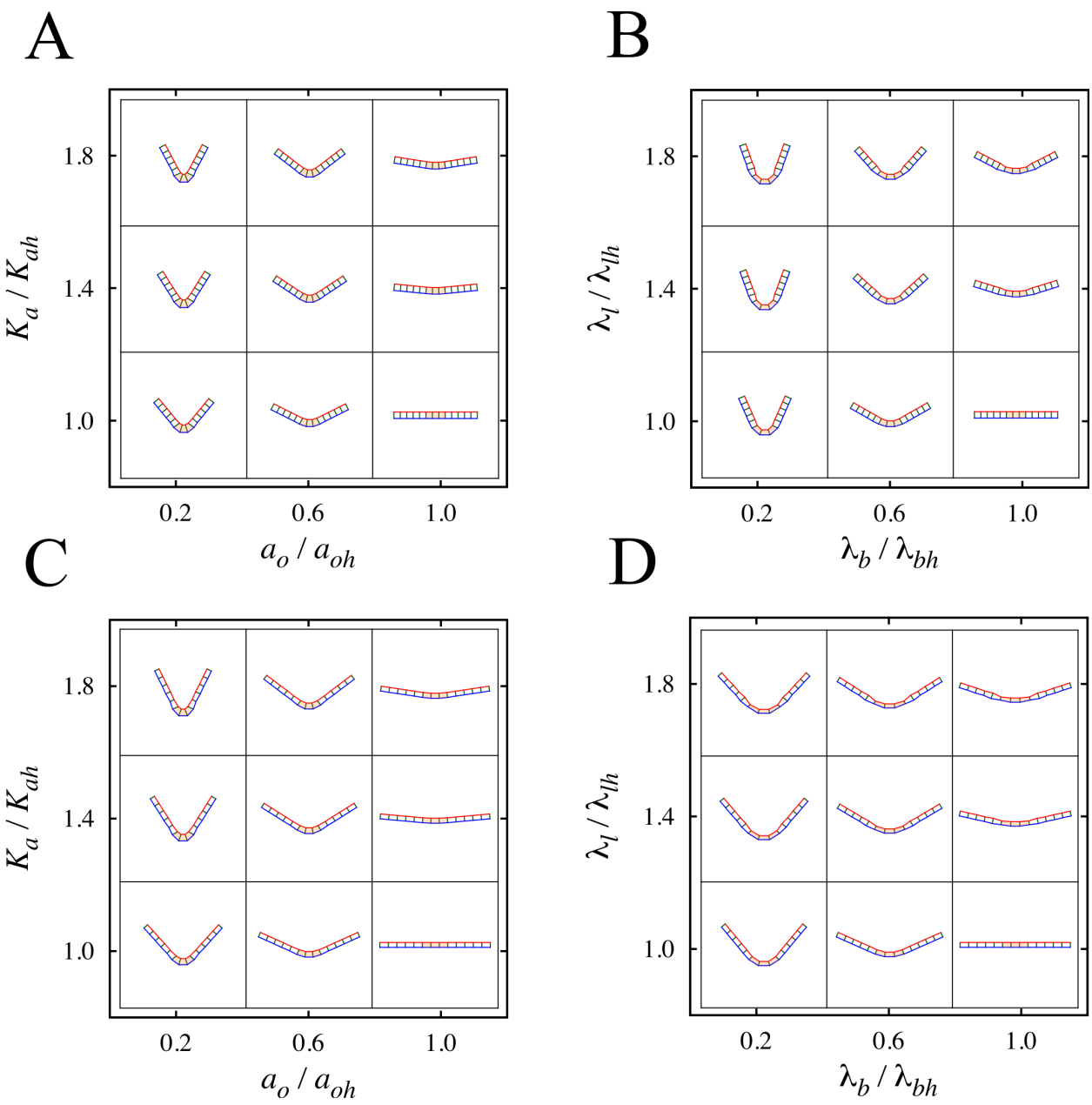

FIG. S5. Fold formation in cell sheets ($N = 13$) comprising cuboidal ($g = 1$, Top) or squamous cells ($g = 1.75$, Down). The central cells ($N_c = 3$, colored by orange) actively change their mechanical properties (a_o, K_a, λ_b, λ_ℓ), while the mechanics of surrounding cells (a_{oh}, K_{ah}, λ_{bh}, $\lambda_{\ell h}$) remain unchanged. The homogeneous sheet on the lower-right corner is generated with parameter values $(K_a, a_o, \lambda_b, \lambda_\ell) = (0.25, 0.746, 0.1, 0.1)$ (Top) and $(0.143, 0.986, 0.076, 0.133)$ (Down).